THE EUROPEAN
PHYSICAL JOURNAL C

CrossMark

Is the proton radius puzzle evidence of extra dimensions?

F. Dahia[a], **A. S. Lemos**

Department of Physics, Universidade Federal da Paraíba, João Pessoa, PB, Brazil

Abstract The proton charge radius inferred from muonic hydrogen spectroscopy is not compatible with the previous value given by CODATA-2010, which, on its turn, essentially relies on measurements of the electron–proton interaction. The proton's new size was extracted from the 2S–2P Lamb shift in the muonic hydrogen, which showed an energy excess of 0.3 meV in comparison to the theoretical prediction, evaluated with the CODATA radius. Higher-dimensional gravity is a candidate to explain this discrepancy, since the muon–proton gravitational interaction is stronger than the electron–proton interaction and, in the context of braneworld models, the gravitational potential can be hugely amplified in short distances when compared to the Newtonian potential. Motivated by these ideas, we study a muonic hydrogen confined in a thick brane. We show that the muon–proton gravitational interaction modified by extra dimensions can provide the additional separation of 0.3 meV between the 2S and 2P states. In this scenario, the gravitational energy depends on the higher-dimensional Planck mass and indirectly on the brane thickness. Studying the behavior of the gravitational energy with respect to the brane thickness in a realistic range, we find constraints for the fundamental Planck mass that solve the proton radius puzzle and are consistent with previous experimental bounds.

1 Introduction

The proton charge radius was determined with unprecedented precision by recent measurements of the Lamb shift in muonic hydrogen [1,2], the atom formed by a muon and a proton (μp). It happens that the deduced radius $r_p = 0.84184(67)$ fm is 4 % smaller than CODATA-2010 value, $r_p^{CD} = 0.8775(51)$ fm [3] — which is inferred from hydrogen and deuteron spectroscopy [4–11] and from measurements of differential cross section in elastic electron–proton

scattering [12–14]. This discrepancy of 7 standard deviations is known as the proton radius puzzle.

The proton charge radius is defined as $\langle r_p^2 \rangle = \int r^2 \rho_E (\mathbf{r}) d^3\mathbf{r}$, where ρ_E is the normalized electric charge density of the proton. Based on the standard theory of bound-state quantum electrodynamics (QED), the effects of the proton internal structure on the atomic energy spectrum can be predicted. For instance, in the muonic hydrogen, it is expected that the contribution for the $2S_{1/2}$–$2P_{1/2}$ Lamb shift is given by [2, 15]

$$\Delta E_L^{th} = \left[206.0668(25) - 5.2275(10) \frac{r_p^2}{\text{fm}^2} \right] \text{meV} \qquad (1)$$

where r_p must be expressed in femtometer. According to this formula, the energy shift is $\Delta E_L^{th} \left(r_p^{CD} \right) = 202.0416(469)$ meV, when it is calculated with the CODATA-2010 radius. On the other hand, the experimental value is extracted from the measurement of the $(2P_{3/2}^{F=1} - 2S_{1/2}^{F=0})$ and $(2P_{3/2}^{F=2} - 2S_{1/2}^{F=1})$ transitions frequencies, ν_s and ν_t, respectively, and from the formula [2,15]

$$\Delta E_L^{\exp} = \frac{1}{4}h\nu_s + \frac{3}{4}h\nu_t - 8.8123 \,(2) \text{ meV}, \qquad (2)$$

where the numeric term comes from the explicit calculation of the 2P fine and hyperfine splitting. By using the measured frequencies, $\nu_s = 54611.16\,(1.05)$ GHz [2,15] and $\nu_t = 49881.35(65)$ GHz [1,2,15], we find $\Delta E_L^{\exp} = 202.3706(23)$ meV. The difference of 0.3290(469) meV, between the measured Lamb shift and the predicted value, has no explanation within the standard framework of physics. Thus the puzzle may be an indication of a missing term in Eq. (1), associated with an unknown proton–muon interaction that differs from the electron–proton interaction. New interactions beyond the standard model have been proposed to explain the energy excess [16–29], but there is no final conclusion yet.

[a] e-mail: fdahia@fisica.ufpb.br

Springer

Here we want to discuss an alternative explanation. As the muon is around 207 times heavier than the electron, it is reasonable to conjecture that gravity is the missing piece in this puzzle. The problem is that the Newtonian potential is negligible in atomic system. However, in the context of the braneworld with a large extra dimension, the gravitational potential can be much greater in short distances. This fact has motivated us to address this issue in the context of the braneworld models.

In the braneworld scenario, our visible Universe is a submanifold with three spatial dimensions (the 3-brane) embedded in an ambient space of higher dimensions (the bulk) [30–33]. Matter and standard model fields are confined to the brane while gravity can propagate in every direction of the bulk. Although gravity has access to whole ambient space, the existence of a bound zero-mode (due to a compact topology or to an appropriate curvature of the bulk), guarantees that the Newtonian behavior is recovered for distances greater than a characteristic length scale ℓ of the extra space, making the model phenomenologically viable. In the case of a compact topology, ℓ is the size of the supplementary space, while in the case of non-compact topology, ℓ is related to the curvature radius of the ambient space. It follows from this picture that gravity may feel directly the effects of extra dimensions in a length scale that could be much greater than the scale in which matter and other fields experience the influence of extra dimensions.

Tests of the inverse square law in laboratory establish that the radius of the extra dimension should be smaller than 44 μm [34–38]. This is the tightest constraint for models with only one extra dimension. When the number of extra dimensions is greater, the most stringent constraints come from astrophysics [39,40] and high energy particle collisions [41–45].

If the gravitational field obeys the Gauss law in the bulk, in the weak field limit, then the gravitational potential of a point-like mass behaves as $(G_n m)/r^{n+1}$ for $r << \ell$, where G_n is the gravitational constant defined in a space with n extra dimensions. The relation between the Newtonian constant, G, and G_n is given by $G_n \sim G\ell^n$, in magnitude order. Therefore, in comparison with the Newtonian potential, the extra-dimensional version is amplified by a factor of the order of $(\ell/r)^n$ in short distances. This property has motivated the study of the gravitational interaction in atomic and molecular systems as a way of obtaining empirical bounds for the number and size of the extra dimensions [46–53]. Considering that the gravitational interaction is a small term of the atomic Hamiltonian, we find that the gravitational energy is proportional to the mean value of $r^{-(n+1)}$ in the atomic state. However, this average diverges for S-states, when $n > 2$. To avoid this problem, some authors introduce a cut-off radius to perform the calculations [46–51]. As a consequence, the results become dependent on an arbitrary parameter. Previ-

ous attempts of solving the proton radius puzzle by means of the extra-dimensional gravity also resorted to a cut-off radius [49,50].

In a thick brane scenario the divergence problem is naturally solved. The origin of the divergences is the fact that a delta-like confinement in the brane is a singular distribution from the viewpoint of the bulk [53,54]. However, in a thick brane scenario, the confined particles are described by a regular wave function with a non-null width in the transversal directions. This width should be less than the brane thickness and its value is related to the strength of the confinement. As the width is non-null, the divergence problem naturally disappears.

Considering the muonic hydrogen in this scenario, we find the energy shift of the atomic states caused by the muon–proton gravitational interaction. Based on these calculations, we show that the gravitational energy can account for the energy excess of the measured Lamb shift, solving, in this way, the proton radius puzzle. This condition determines some constraints for the higher-dimensional Planck mass which are consistent with previous empirical bounds.

2 The gravitational energy of an atom in a thick brane

In the field-theory framework, the brane can be seen as a topological defect capable of trapping matter inside its core [55]. As an illustration, we can mention a domain wall in (4+1) dimensions that separates two vacuum states of a scalar field ϕ along the extra dimension z [55]. In this configuration, the scalar field can confine matter in the center of the wall by means of a Yukawa-type interaction with Dirac spinors. Under the influence of this interaction, the zero-mode state is described by the following wave function:

$$\Psi(\mathbf{x}, z) = \exp\left[-\beta \int_0^z \phi_0(y)\, \mathrm{d}y\right] \psi(\mathbf{x}),\qquad (3)$$

where β is the coupling constant, $\psi(\mathbf{x})$ represents a free spinor in the $(3+1)$ dimensions, $\phi_0 = \eta \tanh(z/\varepsilon)$ is the scalar in a domain wall configuration interpolating between two vacua $\pm\eta$ of the scalar field. This wave function has a peak at the center of the brane ($z = 0$) and decreases exponentially in the transverse direction. The parameter ε can be seen as a measure of the brane thickness, which must be smaller than 10^{-19} m to be consistent with current experimental constraints [30,42,43].

The confinement mechanism for matter in topological defects of greater codimension can be formulated in a similar away. Based on the previous example, it is reasonable to expect that the wave function of localized particles can be written as $\Psi(\mathbf{r}, \mathbf{z}) = \chi(\mathbf{z}) \psi(\mathbf{r})$, where $\chi(\mathbf{z})$ is some

normalized function defined in the supplementary space of n dimensions, concentrated around the origin.

In this context, let us now study the gravitational potential produced by a confined particle in the thick brane. As we are assuming that $\ell >> \varepsilon$, then we have to consider the direct effects of the extra dimensions on the gravitational potential. To take this into account, we will admit that the static gravitational field satisfies the Gauss law in the bulk. Thus, in the case of a flat supplementary space with a compact topology, the exact potential of a point-like mass M lying in the origin of the coordinate system and evaluated at the position $\mathbf{R} = (\mathbf{r}, \mathbf{z})$ can be written [56]

$$V(\mathbf{R}) = -\frac{G_n M}{R^{n+1}} - \sum_i \frac{G_n M}{|\mathbf{R} - \mathbf{R}_i'|^{n+1}}, \tag{4}$$

where the sum spans the topological images of M in the covering space of the extra-dimensional manifold and $R = |\mathbf{R}|$. The exact position $\mathbf{R}_i'$ of the mirror images depends on the topology of the supplementary space. For instance, in the case of a flat n-torus with size ℓ, we have $\mathbf{R}_i = \ell(0, 0, 0, \mathbf{k}_i)$, where $\mathbf{k}_i$ is a vector with n integer number as components. The gravitational potential (4) reduces to the Newtonian potential $-GM/r$ in the far zone ($r >> \ell$) [56].

Regarding the influence of the gravitational potential on the energy spectrum of the muonic hydrogen, the topological images can be neglected, since the contribution they give is lesser than the empirical error of the μp experiment (see the appendix). Therefore, to calculate the proton gravitational potential, ϕ, we may use the approximate Green function $-GM/R^{n+1}$, which is weaker than the real potential of a point-like mass. So, assuming that the proton mass m_p is distributed on the spatial extension of the nucleus, the proton gravitational potential is

$$\phi(\mathbf{R}) = -G_n \int \frac{\rho_M(\mathbf{R}')}{|\mathbf{R} - \mathbf{R}'|^{n+1}} \mathrm{d}^{3+n}\mathbf{R}', \tag{5}$$

where the mass density is $\rho_M = |\Psi_p|^2 m_p$ and $\Psi_p(\mathbf{r}, \mathbf{z}) = \chi_p(\mathbf{z})\psi_p(\mathbf{r})$ is the higher-dimensional wave function of the proton.

The muon–proton gravitational interaction, which is described by the Hamiltonian $H_G = m_\mu \phi$ (where m_μ is the muon mass), modifies the muonic hydrogen spectrum. Assuming that H_G is a small term of the atomic Hamiltonian, the energy shift can be calculated by the perturbation method for each state. In the first order, the energy correction is $\langle m_\mu \phi \rangle_\Psi$, i.e., the mean value of the gravitational energy in the state Ψ. By using Eq. (5), we can write the energy shift

$$\delta E_\psi^g = -G_n m_p m_\mu \int \frac{|\Psi_p|^2 |\Psi_\mu|^2}{|\mathbf{R} - \mathbf{R}'|^{n+1}} \mathrm{d}^{3+n}\mathbf{R}\,\mathrm{d}^{3+n}\mathbf{R}', \tag{6}$$

where the higher-dimensional wave function of the muon (more precisely, the reduced particle) $\Psi_\mu(\mathbf{r}, \mathbf{z})$ is the product of the extra-dimensional part $\chi_\mu(\mathbf{z})$ and the solutions $\psi_\mu(\mathbf{r})$ of the Schrödinger equation for the muonic hydrogen.

To calculate (6), we shall assume that the proton mass is uniformly distributed inside the nucleus. This means that the three-dimensional part, $\psi_p(\mathbf{r})$, is constant in the spatial extension of the nucleus and zero outside $\left(r > r_p^{CD}\right)$. In Eq. (6), the major contribution comes from the integral in the interior region of the nucleus. For S-states, Eq. (6) yields

$$\delta E_S^g = -\gamma_n \frac{G_n m_p m_\mu}{\sigma^{n-2}} |\psi_S(0)|^2 \left[1 - \frac{3}{2}\frac{r_p}{a_0} + O\left(r_p^2/a_0^2\right) \right]$$
$$\times \left[1 + O\left(\sigma/r_p\right) \right], \tag{7}$$

where a_0 is the Bohr radius of the muonic hydrogen, $\psi_S(0)$ is the wave function of a S-state evaluated in the origin and γ_n is a numeric factor whose value depends on the number of extra dimensions. For instance, $\gamma_3 = 2\pi^{3/2}$, $\gamma_4 = 4\pi/3$, $\gamma_5 = \pi^{3/2}/3$ and $\gamma_6 = 4\pi/15$. The gravitational energy depends on how tight the confinement in the thick brane is. In fact, σ is associated to the spatial distribution of the particles in the transverse direction. This parameter is defined by

$$\frac{1}{\sigma^m} \equiv \frac{\Gamma(n/2)}{\Gamma\left(\frac{n-m}{2}\right)} \int \frac{|\chi_p(\mathbf{z}_1)|^2 |\chi_\mu(\mathbf{z}_2)|^2}{|\mathbf{z}_1 - \mathbf{z}_2|^m} \mathrm{d}^n\mathbf{z}_1 \mathrm{d}^n\mathbf{z}_2, \tag{8}$$

where m is a positive integer that should satisfy the condition $m \leq (n-1)$ and Γ stands for the gamma function. If χ is a Gaussian function, then σ coincides with the standard deviation of the Gaussian distribution. For the sake of consistency, σ should be smaller than the brane thickness.

Equation (7) is valid for $n > 2$. Here we do not discuss the cases $n = 1$ and $n = 2$, once the atomic gravitational energy are not strong enough to explain the proton radius puzzle in those dimensions. The integral of Eq. (6) in the external region is smaller than (7) by a factor of the order of σ/r_p, which is lesser than 10^{-5} for realistic branes with $\varepsilon \leq 10^{-20}$ m. On its turn, for P-states, the gravitational contribution is smaller than (7) by a factor of the order of r_p^2/a_0^2.

3 The additional energy in the Lamb shift

As we have already mentioned, in comparison with the predicted Lamb shift $\Delta E_L^{th}\left(r_p^{CD}\right)$, the measured value ΔE_L^{exp} has an excess of 0.3290(469) meV. The higher-dimensional gravity can explain this excess in a consistent way. Due to the gravitational proton–muon interaction, the energy of the $2S$-level decreases by the amount $\delta E_{2S}^g = -\gamma_n G_n m_p m_\mu \left(1 - 3r_p/2a_0\right)/(8\pi a_0^3 \sigma^{n-2})$, according to Eq. (7). On the other hand, the effect on the $2P$-level is
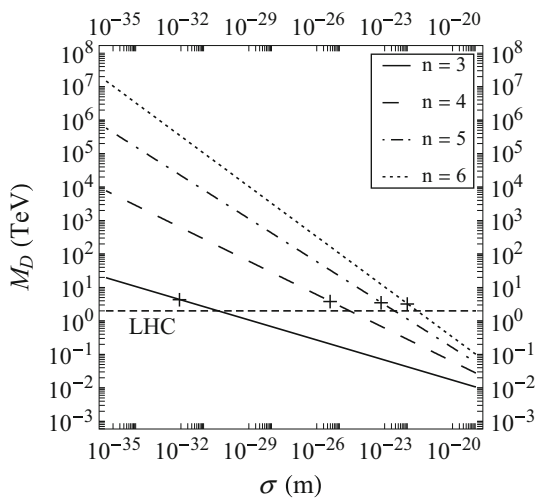
Fig. 1 The required values of higher-dimensional Planck mass (in natural units) to explain the proton radius puzzle, in terms of the confinement parameter σ. The region below the 2 TeV line is excluded from the analysis of monophoton events in proton–proton collision at LHC. The + signs are lower bounds from data on the monojet events at LHC

smaller by a factor of the order of 10^{-5}; therefore, it is negligible within the precision of 10^{-7} eV of the muonic hydrogen experiment [15]. Thus, the gravitational interaction is responsible for an additional enlargement between the $2P$ and $2S$ levels given by $\left|\delta E_{2S}^g\right|$. The puzzle would be solved if $\left|\delta E_{2S}^g\right| = 0.3290(469)$ meV. This condition implies a relation between G_n and σ, which, in terms of the fundamental Planck mass M_D of the higher-dimensional space, as defined in Ref. [41], can be written

$$\left[\frac{(\hbar/c)^n \hbar c}{(n+2)} \frac{\Gamma\left(\frac{n+3}{2}\right)}{2\pi^{(n+3)/2}} \frac{(2\pi)^n}{M_D^{n+2}} \right] \frac{\gamma_n}{8\pi} \frac{m_p m_\mu}{a_0^3 \sigma^{n-2}} \left(1 - \frac{3r_p}{2a_0}\right)$$
$$= 0.3290(469) \text{ meV}, \tag{9}$$

where G_n was substituted by the term in the bracket. Figure 1 shows a numerical analysis of Eq. (9) for four cases $n = 3, 4, 5$ and 6. The constraints yield the required values of M_D, in the range 10^{-35} m $\leq \sigma \leq 10^{-20}$ m, in order to solve the proton radius puzzle. As we can see, thinner branes—which imply tighter confinements, i.e., smaller σ—require higher values for the fundamental Planck mass. The uncertainty on the higher-dimensional Planck mass at 1 standard deviation level is $\delta M_D/M_D = 0.1426/(n+2)$ for fixed σ, and it is too narrow to be seen in Fig. 1.

Let us now compare these constraints with other experimental bounds. Direct tests on deviation of the inverse square law at short distances, based on modern versions of torsion-balance instrument, have been used with the purpose of searching for signals of extra dimensions. In these experiments, the modified gravitational potential is parameterized as $GM/r\left(1 + \alpha e^{-r/\lambda}\right)$, where, in the ADD model, $\alpha = 8n/3$ and λ is equal to the radius R of the extra dimensions

[35–38]. From the empirical constraints on α and λ, upper bounds for R are inferred for each value of n. For instance, for $n = 1$ and $n = 2$, the data imply that $R < 44\mu$m and $R < 37\mu$m, respectively, which corresponds (see, the relation between R and M_D in the appendix) to $M_D > 3.6$ TeV for $n = 2$ [37,57]. For greater codimensions, the experimental limits are much below than TeV scale and, therefore, compatible with constraints of Fig. 1. If the modification of the gravitational potential is due to radion exchange between matter, instead of graviton exchange, the parameters have different meaning. In this case, $\alpha = n/(n+2)$ and λ is the Compton wavelength of the radion, which is related to M_* (the unification scale [58]) by the formula $\lambda^2 \sim \left(\hbar^3/cGM_*^4\right)$ [58–60]. According to Ref. [58], the limits go from $M_* > 5.7$ TeV ($n = 1$) to $M_* > 6.4$ TeV ($n = 6$). Although the exact relation between λ and the fundamental Planck mass depends on the stabilization mechanism of the radion [60], there is plenty of space to accommodate these bounds in Fig. 1, for $n > 3$.

Astrophysical and cosmological constraints are strong for $n \leq 4$ and are derived from the implications of the supposed production of the KK gravitons in stars [39,40,57,61]. In this context, the most stringent bound is obtained from the analysis of this process in supernovae explosions. In the ADD higher-dimensional model, an old remnant neutron star is surrounded by trapped KK gravitons which slowly decay into photons. A fraction of them is absorbed by the neutron star causing its heating. As the excess heat is not observed, constraints can be obtained. Data from PSR J09521 + 0755 demand that $M_D > 76$ TeV for $n = 3$ [40,57]. In principle, this limit would rule out the case $n = 3$ of our analysis in Fig. 1. However, it is important to have in mind that astrophysics bounds could be evaded by some mechanism that provides an extra mass for KK gravitons [61–64].

When the number of extra dimensions is greater than four, the tightest constraints of the fundamental Planck mass comes from high-energy collisions. Recent analysis on monophoton events in proton–proton collision at $\sqrt{s} = 7$ TeV and $\sqrt{s} = 8$ TeV in the LHC [42,43] determines that $M_D > 2$ TeV, for $n = 3, \ldots, 6$. In Fig. 1, this lower bound is represented by the horizontal line. On its turn, the analysis of monojet events in proton–proton collision at $\sqrt{s} = 8$ TeV provides stronger constraints. Considering the LO cross section for direct graviton emission in the collision, the lower bounds for M_D in TeV are: 4.38 ($n = 3$), 3.86 ($n = 4$), 3.55 ($n = 5$), and 3.26 ($n = 6$) [44,45]. The bounds are indicated in Fig. 1 by a + sign. Above these values, constraints of Fig. 1 are compatible with the collider limits too.

Finally let us now compare our results with other spectroscopy data. In a previous work [53], considering a hydrogen stuck in a thick brane, we determined lower bounds for the higher-dimensional Planck mass from the $2S$–$1S$ transition. The limits from H spectroscopy are weaker than those necessary to solve the proton radius puzzle. This means that,

considering the current constraints of M_D as shown in Fig. 1, the gravitational energy is capable of explaining the additional difference between the $2S_{1/2}$ and $2P_{1/2}$ states of μp, but it is still hidden in the H spectrum. The reason is that, according to Eq. (7), the atomic energy due to the gravitational interaction depends on the lepton mass to the fourth order, m^4, approximately, since the energy is proportional to m/a_0^3 and a_0 is defined in terms of atomic reduced mass. Thus, the gravitational energy of the hydrogen is almost $(200)^4$ times smaller than that of μp, assuming that the confinement of both atoms is similar, i.e., $\sigma_H \simeq \sigma_{\mu p}$. Therefore, the constraints from the muonic hydrogen are also compatible with the most precise spectroscopic data available, which is provided by the hydrogen spectrum.

So, based on these considerations, we can conclude that there are regions in Fig. 1 in which the required values of M_D to solve the proton radius puzzle satisfy all previous experimental bounds.

At this point, it is important to emphasize that the calculations we have done here are based on the classical behavior of gravity. However, as pointed out in Ref. [41], quantum-gravity effects may become significant in a length scale of the order of l_D (the Planck length defined in the higher-dimensional space, which is given by $l_D = (\hbar/c) M_D^{-1}$) or even in a greater scale, depending on the fundamental theory of gravity, not yet known. If this is the case, then unpredicted phenomena could distort or even overshadow the classical effects we have investigated here.

However, according to [65], if the theory of General Relativity is considered as an effective theory, then it is possible to estimate quantum corrections to the gravitational potential energy. In three-dimensional space, if d is the distance between particles with mass M and m, then the classical potential energy is given by the Newtonian term GMm/d and quantum contributions are smaller by a factor of the order of $\left(l_p/d\right)^2$, where l_p is the usual Planck length. In the higher-dimensional case, the classical term is $G_n Mm/d^{n+1}$, and, according to dimensional analysis, the quantum corrections would be of the order of $(l_D/d)^{n+2}$. Of course, in the muonic hydrogen, proton and muon cannot be considered as point-like particles. Nevertheless, it is instructive to define an effective distance between them, in the extra-dimensional space, d_{eff}, by writing the atomic gravitational energy as $G_n m_p m_\mu / d_{\text{eff}}^{n+1}$. Now, from Eq. (9), d_{eff} can be estimated. Comparing it with the fundamental Planck length, we verify that the ratio $(l_D/d_{\text{eff}})^{n+2}$ depends on n and σ, but, for any dimension and for any value of σ investigated here, it is smaller than 10^{-4}. Thus, if d_{eff} is the relevant characteristic length scale of the system concerning its gravitational interaction, then we can expect that the classical contribution will be the leading gravitational influence in this system within the braneworld scenario we are considering here. However,

as the fundamental quantum-gravity theory is not known, only experiments can answer this question.

4 Final remarks

In the thick brane scenario, the direct influence of extra dimensions on gravity arises in a length scale ℓ that may be much greater than the scale in which standard model fields feel directly the effects of supplementary space. It happens that the modified gravitational potential is amplified in small distances ($r << \ell$) when compared to the Newtonian potential. In this context, we found that the proton–muon gravitational interaction can explain the excess of 0.3 meV in the Lamb shift of muonic hydrogen, provided that the fundamental Planck mass satisfies some constraints. In Fig. 1, we can find constraints for M_D which solve the proton radius puzzle without violating any previous empirical bound.

In the muonic hydrogen experiment, the 2S hyperfine splitting (2S-HFS) was investigated too [15]. In the leading order, the proton structure affects 2S-HFS by means of the so-called Zemach radius, which is defined in terms of the convolution between the electric and magnetic distribution of proton. Within the current precision, the gravitational energy does not change 2S-HFS. This result is consistent with the fact that measurements of Zemach radius extracted from the muonic hydrogen and from H spectroscopy are compatible.

The proton radius puzzle may be the first empirical evidence of the existence of hidden dimensions. In view of this exciting implication, the model must be tested further. It is important to investigate the theoretical predictions for other transitions. As an example, let us mention the $2S$–$1S$ transition. In the muonic hydrogen, there is expected an extra energy of 2.1 meV in this transition. On its turn, in the electronic hydrogen, assuming that $\sigma_H \simeq \sigma_{\mu p}$, this model predicts that the $2S$–$1S$ transition frequency should exhibit an excess of 420 Hz, which is greater than the experimental error of 10 Hz [4]. In spite of this, the extra-dimensional effect is still hidden in H spectroscopy because of uncertainties related to the measurement of the proton radius, which corresponds to 32 kHz [66]. Thus, to reveal the traces of extra dimensions in the $2S$–$1S$ transition of the hydrogen, the precision of r^{CD} should be improved.

In contrast with other alternatives, a distinguishable characteristic of this model is the universality of the effects. All atoms are affected by extra dimensions through the modification of the gravitational interaction. Moreover, in the case of hydrogen-like atoms, Eq. (7) predicts a peculiar dependence of the gravitational energy on the mass of the atomic particles. The energy shift of any S-state is proportional to $(Mm)^4 / (m + M)^3$, where M is the nucleus mass and m is the mass of the orbiting particle. Assuming the confine-

ment in the brane is similar for all atoms, we can estimate the energy shift caused by extra dimensions in any exotic hydrogen-like atom. Experimental confirmation of the predicted behavior could be an indication of the existence of extra dimensions.

Appendix

Let us consider Eq. (4). Here we want to demonstrate that the potential generated by the topological images, V_{im}, is negligible within the μp experiment precision. The value of V_{im} depends on the point $\mathbf{R} = (\mathbf{r}, \mathbf{z})$. We obtain an upper bound for $|V_{im}|$ by evaluating each term of the series in an appropriate point $\mathbf{R}_{min}$ of the ambient space of least distance from the corresponding topological image (located in the covering space). First, notice that for all the points $\mathbf{R}_{min}$, we should have $\mathbf{r} = 0$. Thus,

$$|V_{im}| = \sum_i \frac{G_n M}{|\mathbf{R} - \mathbf{R}'_i|^{n+1}} \leq \sum_i \frac{G_n M}{|\mathbf{z} - \ell \mathbf{k}_i|^{(n+1)}}. \tag{10}$$

If the supplementary space is a flat n-torus with sides of length ℓ, then $-\ell/2 \leq z_i \leq \ell/2$. Let us consider that the real mass M is in the center of this space, which we will denote by $T_0(\ell)$. The covering space, $\mathbb{R}^n$, can be viewed as if it were filled by cells that are copies of $T_0(\ell)$. Now consider a mirror image i of M that belongs to another cell. We want to determine the least distance from i to $T_0(\ell)$. Notice that the fundamental cell $T_0(\ell)$ is inside a ball B of radius $d = \sqrt{n}\ell/2$ (the semi-diagonal of $T_0(\ell)$). For $n < 8$, only the first neighbors, whose distance to the center of $T_0(\ell)$ is ℓ, are inside this ball. And, with respect to them, the least distance to $T_0(\ell)$ is $\ell/2$.

Now let us consider images which are outside B. The distance from i, whose position is $\ell \mathbf{k}_i$, to any point of $T_0(\ell)$ is greater than the radial distance from i to the surface of B, i.e., $|\mathbf{z} - \ell \mathbf{k}_i| \geq \ell k_i - d$, for any $\mathbf{z} \in T_0$ and $k_i = |\mathbf{k}_i| > 1$. Therefore, $\ell k_i - d$ is a lower estimate of the least distance from i to $T_0(\ell)$. There are $2n$ images with $k_i = 1$. The next neighbors have $k_i = \sqrt{2}$. Thus, separating the contributions from first neighbors ($k_i = 1$), we may write

$$|V_{im}| \leq \frac{2n G_n M}{(\ell/2)^{n+1}} + \frac{G_n M}{\ell^{n+1}} \sum_{k_i \geq \sqrt{2}} \frac{1}{\left(k_i - \sqrt{n}/2\right)^{(n+1)}}. \tag{11}$$

To estimate this quantity, let us define $T_i(1)$—the symmetric n-torus of unity size with center at the image i. Each term within the summation sign can be interpreted as the volume of a column above $T_i(1)$ and whose height is given by the step function $f(k_i) \equiv \left(k_i - \sqrt{n}/2\right)^{-(n+1)}$. Now we introduce the continuous function $g(x) = \left(x - \sqrt{n}\right)^{-(n+1)}$, where $\mathbf{x}$ is the position vector in the covering space. The semi-diagonal of $T_i(1)$ measures $\sqrt{n}/2$. Therefore, for every $\mathbf{x} \in T_i(1)$, $x \leq \left(k_i + \sqrt{n}/2\right)$. Now, as $g(x)$ is a decreasing function, then $g(x) \geq g\left(k_i + \sqrt{n}/2\right) = f(k_i)$ inside the cell $T_i(1)$. Thus, the integral of $g(x)$ in the region $T_i(1)$ is an upper estimate for $f(k_i)$. For the sake of consistency, we should have $x > \sqrt{n}$, according to the definition of $g(x)$. On the other hand, as $x \geq \left(k_i - \sqrt{n}/2\right)$ for $x \in T_i(1)$, then we may conclude that the previous analysis are valid for $k_i > 3\sqrt{n}/2$, i.e., only for cells whose center is separated from the origin by a distance greater than $3\sqrt{n}/2$. A possible choice is $k_i = 2\sqrt{n}$. Closer cells should be taken separately. Thus, computing the contributions given by the first neighbors ($k_i = 1$), by the images at intermediary positions $\left(\sqrt{2} \leq k_i \leq 2\sqrt{n}\right)$ and from the most distant images $\left(k_i > 2\sqrt{n}\right)$, we may write the potential V_{im}

$$|V_{im}| \leq \frac{G_n M}{\ell^{n+1}} \left(2^{n+2} n + \sum_{\sqrt{2} \leq k_i \leq 2\sqrt{n}} \frac{1}{\left(k_i - \sqrt{n}/2\right)^{(n+1)}} \right.$$
$$\left. + \frac{1}{n^{3/2}} \frac{2\pi^{n/2}}{\Gamma(n/2)} \left(3^n - 1\right) \right), \tag{12}$$

where we have employed the following estimation:

$$\sum_{k_i > 2\sqrt{n}} \frac{1}{\left(k_i - \sqrt{n}/2\right)^{(n+1)}} \leq \int_{x > 3\sqrt{n}/2} \frac{d^n\mathbf{x}}{\left(x - \sqrt{n}\right)^{(n+1)}}$$
$$= \frac{1}{n^{3/2}} \frac{2\pi^{n/2}}{\Gamma(n/2)} \left(3^n - 1\right). \tag{13}$$

Therefore, in the case of muonic hydrogen, the gravitational energy due to the topological images is less than $\left(G_n m_p m_\mu / \ell^{n+1}\right) F_n$, where F_n is the function defined from (12), which depends only on the number of extra dimensions and that can be explicitly calculated for $n < 8$. In magnitude order, $G_n \sim G\ell^n$; then, in terms of the Newtonian gravitational constant, we may write $|V_{im}| \leq \left(G m_p m_\mu / \ell\right) \tilde{F}_n$. As the precision of the muonic hydrogen experiment is 10^{-7} eV, the effect of the topological images would be detectable only if $\ell \lesssim 10^{-36}$ m. However, as we shall see, the order of ℓ is much greater according to our constraints. To verify this, let us estimate the size of the extra dimensions. The relation between ℓ and the higher-dimensional Planck mass (M_D^{2+n}) is given by $G^{-1} = 8\pi \mathcal{R}^n \mathcal{M}_D^{2+n}$, where $\mathcal{R} = (\ell/2\pi)$ is the radius of the extra dimensions and $\mathcal{M}_D^{2+n} = M_D^{2+n} / [(\hbar/c)^n \hbar c]$. This relation allows us to estimate the size of extra dimensions from the constraints of M_D
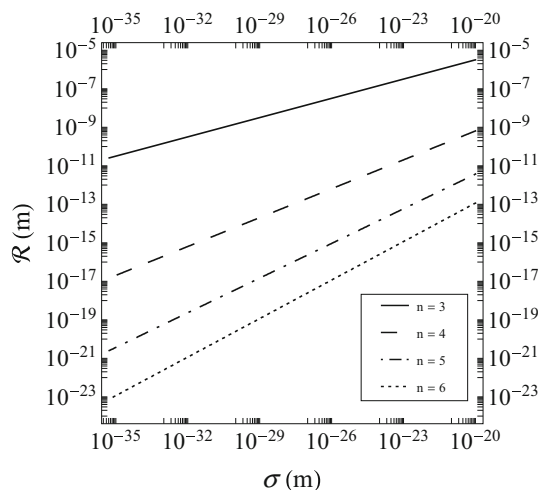
Fig. 2 Constraints for the radius ($\mathcal{R} = \ell/2\pi$) of the supplementary space (a flat n-torus) in terms of the confinement parameter σ

given by Fig. 1. Empirical bounds for the torus radius ($\ell/2\pi$) in the cases $n = 3, \ldots, 6$ are shown in Fig. 2. By using these values, we can explicitly check that the contribution of the topological images is negligible indeed.

References

1. R. Pohl et al., Nature **466**, 213 (2010)
2. A. Antognini et al., Science **339**, 417 (2013)
3. P.J. Mohr, B.N. Taylor, D.B. Newell, Rev. Modern Phys. **84**, 1527 (2012)
4. C.G. Parthey et al., Phys. Rev. Lett. **107**, 203001 (2011)
5. B. de Beauvoir, C. Schwob, O. Acef, L. Jozefowski, L. Hilico, F. Nez, L. Julien, A. Clairon, F. Biraben, Eur. Phys. J. D **12**, 61 (2000)
6. S.R. Lundeen, F.M. Pipkin, Phys. Rev. Lett. **46**, 232 (1981)
7. E.W. Hagley, F.M. Pipkin, Phys. Rev. Lett. **72**, 1172 (1994)
8. C. Schwob et al., Phys. Rev. Lett. **82**, 4960 (1999)
9. M. Fischer et al., Phys. Rev. Lett. **92**, 230802 (2004)
10. C.G. Parthey, A. Matveev, J. Alnis, R. Pohl, T. Udem, U.D. Jentschura, N. Kolachevsky, T.W. Hänsch, Phys. Rev. Lett. **104**, 233001 (2010)
11. O. Arnoult, F. Nez, L. Julien, F. Biraben, Eur. Phys. J. D **60**, 243 (2010)
12. I. Sick, Phys. Lett. B **576**, 62 (2003)
13. P.G. Blunden, I. Sick, Phys. Rev. C **72**, 057601 (2005)
14. J.C. Bernauer et al., Phys. Rev. Lett. **105**, 24200 (2010)
15. A. Antognini et al., Ann. Phys. **331**, 127 (2013)
16. U.D. Jentschura, Ann. Phys. **326**, 516 (2011)
17. P. Brax, C. Burrage, Phys. Rev. D **83**, 035020 (2011)
18. J.I. Rivas, A. Camacho, E. Göklü, Phys. Rev. D **84**, 055024 (2011)
19. S.G. Karshenboim, Phys. Rev. Lett. **104**, 220406 (2010)
20. J. Jaeckel, S. Roy, Phys. Rev. D **82**, 125020 (2010)
21. V. Barger, C.-W. Chiang, W.-Y. Keung, D. Marfatia, Phys. Rev. Lett. **106**, 153001 (2011)
22. D. Tucker-Smith, I. Yavin, Phys. Rev. D **83**, 101702 (2011)
23. B. Batell, D. McKeen, M. Pospelov, Phys. Rev. Lett. **107**, 011803 (2011)
24. V. Barger, C.-W. Chiang, W.-Y. Keung, D. Marfatia, Phys. Rev. Lett. **108**, 081802 (2012)
25. D. McKeen, M. Pospelov, Phys. Rev. Lett. **108**, 263401 (2012)
26. C.E. Carlson, B.C. Rislow, Phys. Rev. D **86**, 035013 (2012)
27. R. Onofrio, Europhys. Lett. **104**, 20002 (2013)
28. P. Brax, C. Burrage, Phys. Rev. D **91**, 043515 (2015)
29. H. Lamm, Phys. Rev. D **92**, 055007 (2015)
30. N. Arkani-Hamed, S. Dimopoulos, G.R. Dvali, Phys. Lett. B **429**, 263 (1998)
31. I. Antoniadis, N. Arkani-Hamed, S. Dimopoulos, G.R. Dvali, Phys. Lett. B **436**, 257 (1998)
32. L. Randall, R. Sundrum, Phys. Rev. Lett. **83**, 3370 (1999)
33. L. Randall, R. Sundrum, Phys. Rev. Lett. **83**, 4690 (1999)
34. J.C. Long, H.W. Chan, J.C. Price, Nucl. Phys. B **539**, 23 (1999)
35. C.D. Hoyle, U. Schmidt, B.R. Heckel, E.G. Adelberger, J.H. Gundlach, D.J. Kapner, H.E. Swanson, Phys. Rev. Lett. **86**, 1418 (2001)
36. C.D. Hoyle, D.J. Kapner, B.R. Heckel, E.G. Adelberger, J.H. Gundlach, U. Schmidt, H.E. Swanson, Phys. Rev. D **70**, 042004 (2004)
37. D.J. Kapner, T.S. Cook, E.G. Adelberger, J.H. Gundlach, B.R. Heckel, C.D. Hoyle, H.E. Swanson, Phys. Rev. Lett. **98**, 021101 (2007)
38. J. Murata, S. Tanaka, Class. Quantum Grav. **32**, 033001 (2015)
39. S. Cullen, M. Perelstein, Phys. Rev. Lett. **83**, 268 (1999)
40. S. Hannestad, G.G. Raffelt, Phys. Rev. D **67**, 125008 (2003) [Erratum-ibid.D, 69, 029901 (2004)]
41. G.E. Giudice, R. Rattazzi, J.D. Wells, Nucl. Phys. B **544**, 3–38 (1999)
42. G. Aad et al. (Atlas Collaboration), Phys. Rev. Lett. **110**, 011802 (2013)
43. G. Aad et al. (CMS Collab.), Phys. Lett. B **755**, 102 (2016)
44. CMS Collab., Eur. Phys. J. C **75**, 235 (2015)
45. G. Landsberg, Mod. Phys. Lett. A **50**, 1540017 (2015)
46. F. Luo, H. Liu, Chin. Phys. Lett. **23**, 2903 (2006)
47. F. Luo, H. Liu, Int. J. Theor. Phys. **46**, 606 (2007)
48. Z.-G. Li, W.-T. Ni, A.P. Patón, Chin. Phys. B **17**, 70 (2008)
49. Z. Li, X. Chen. arXiv:1303.5146 [hep-ph]
50. L.B. Wang, W.T. Ni, Mod. Phys. Lett. A **28**, 1350094 (2013)
51. Z. Wan-Ping, Z. Peng, Q. Hao-Xue, Open Phys. **13**, 96 (2015)
52. E.J. Salumbides et al., N. J. Phys. **17**, 033015 (2015)
53. F. Dahia, A.S. Lemos. arXiv:1509.06817 [hep-ph]
54. F. del Aguila, M. Perez-Victoria, J. Santiago, JHEP **0610**, 056 (2006)
55. V. Rubakov, M. Shaposhnikov, Phys. Lett. B **125**, 136 (1983)
56. A. Kehagias, K. Sfetsos, Phys. Lett. B **472**, 39 (2000)
57. K.A. Olive et al. (Particle Data Group), Chin. Phys. C **38**, 090001 (2014) [Extra dimensions, Updated September 2015 by John Parsons and Alex Pomarol]
58. E.G. Adelberger, B.R. Heckel, S. Hoedl, C.D. Hoyle, D.J. Kapner, A. Upadhye, Phys. Rev. Lett. **98**, 131104 (2007)
59. E.G. Adelberger, B.R. Heckel, A.E. Nelson, Annu. Rev. Nucl. Part. Sci. **53**, 77 (2003)
60. I. Antoniadis, K. Benakli, A. Laugier, T. Maillard, Nucl. Phys. B **662**, 40 (2003)
61. K. Nakamura et al. (Particle Data Group), JPG **37**, 075021 (2010) [Extra dimensions, Updated Sept. 2007 by G.F. Giudice and J.D. Wells]
62. N. Kaloper et al., Phys. Rev. Lett. **85**, 928 (2000)
63. K.R. Dienes, Phys. Rev. Lett. **88**(011601), 9 (2002)
64. G.F. Giudice et al., Nucl. Phys. B **706**, 455 (2005)
65. J.F. Donoghue, Introduction to the effective field theory description of gravity. arXiv:gr-qc/9512024
66. K. Pachucki, U.D. Jentschura, Phys. Rev. Lett. **91**, 113005 (2003)